One-dimensional steady-state photorefractive screening solitons

Konstantine Kos, Hongxing Meng, and Greg Salamo
Physics Department, University of Arkansas, Fayetteville, Arkansas 72701

Ming-feng Shih and Mordechai Segev
Electrical Engineering Department and Advanced Center for Photonics and Optoelectronic Materials (POEM), Princeton University, Princeton, New Jersey 08544

George C. Valley
Hughes Research Laboratories, Malibu, California 90265
(Received 15 November 1995)

We study one-dimensional steady-state photorefractive screening solitons in a bulk strontium barium niobate crystal. We compare measurements and calculations of the soliton properties and find good agreement for relations between the profile, width and intensity of the soliton, the applied voltage and material parameters. We find the solitons stable against perturbations both in the plane and perpendicular to the plane of the soliton for intensities large compared to the background intensity. [S1063-651X(96)50505-2]

PACS number(s): 42.65.Hw, 42.65.Tg

Spatial solitons are a subject of continuing interest in photorefractive materials [1–7]. Since they require very low power and exhibit self-trapping in both transverse dimensions, they have great potential for applications such as beam steering, optical interconnects, and nonlinear optical devices. Photorefractive solitons have been predicted and observed in a quasisteady regime (quasi-steady-state solitons) [1,2], in the steady state in photovoltaic materials (photovoltaic solitons) [3], and in the steady state with an external applied field (screening solitons) [4–6]. Screening solitons occur when an external voltage is applied to a photorefractive crystal such that the internal electric field surrounding a bright beam is screened by the higher conductivity within the beam. The electric field is inversely proportional to the sum of the light intensity and the dark irradiance and is therefore lower in regions of higher optical intensity. This modifies the refractive index via the Pockels effect which for the soliton exactly traps the beam. An observation of steady-state screening solitons trapped in both transverse dimensions was reported earlier this year [6] but theoretical results exist only in one dimension [5–7].

Here we make detailed comparisons between theory and experiments for one-dimensional steady-state screening solitons trapped in a bulk material. The theory predicts a universal relation between the width of the soliton and the ratio of the soliton irradiance to the sum of the equivalent dark irradiance and a uniform background irradiance [5–7]. If the voltage necessary for polarization rotation by π (V_π) is measured separately, there are no free parameters in the theory. We compare this universal relation and the soliton profiles to experimental data and show good agreement. We also observe that the soliton is stable against perturbations both in the plane and perpendicular to the plane of the soliton for intensities large compared to the background intensity.

Previous work [5,7] shows that a one-dimensional (1D) bright screening soliton is described by the reduced wave equation

$$d^2u/d\xi^2+(u/u_0^2)\ln(1+u_0^2)-u/(1+u^2)=0 \qquad (1)$$

whose first integral is

$$du/d\xi=[\ln(1+u^2)-(u^2/u_0^2)\ln(1+u_0^2)]^{1/2} \qquad (2)$$

where $u(\xi)$ is the soliton amplitude (as a function of the transverse coordinate ξ) divided by the square root of the sum of the background and dark irradiances, u_0 is the maximum amplitude of the soliton at $\xi=0$ divided by the same sum, and $\xi=x/d$ where we have the following: $d=(k^2{n_b}^2r_{\rm eff}V/l)^{-1/2}$; $k=2\pi n_b/\lambda$, λ is the free-space wavelength, n_b is the unperturbed refractive index, $r_{\rm eff}$ is the effective electro-optic coefficient for the geometry of propagation, V is the applied voltage, and l is the width of the crystal between the electrodes. Equation (2) can be integrated numerically to obtain the spatial profile of the soliton and the full width at half-maximum (FWHM) of the intensity as a function of u_0.

Solution of Eq. (2) predicts that the narrowest soliton should be obtained for the ratio of peak soliton irradiance to background irradiance about equal to three. We use background intensities of 0.01 to 1 W/cm^2 (much larger than the dark irradiance) which yield one-dimensional solitons of 400 μW of power in a few seconds in SBN:60 (strontium barium niobate). This power is about 600 times larger than that required to generate solitons in two transverse dimensions since the size of the planar soliton is about 10 μm$\times$6 mm rather than about 10 μm$\times$10 μm [6]. Since theoretical results show that soliton profiles depend on the irradiance normalized by the background irradiance, unlike Kerr solitons which depend on absolute irradiance, the irradiance ratio must be kept constant throughout propagation. Because of absorption in the crystal, this means that the soliton and background beam must be roughly copropagating. As in Ref. [6], we generate solitons by launching an extraordinarily polarized focused beam on the background of a uniform, ordinarily polarized, beam both at a wavelength of 514.5 nm and

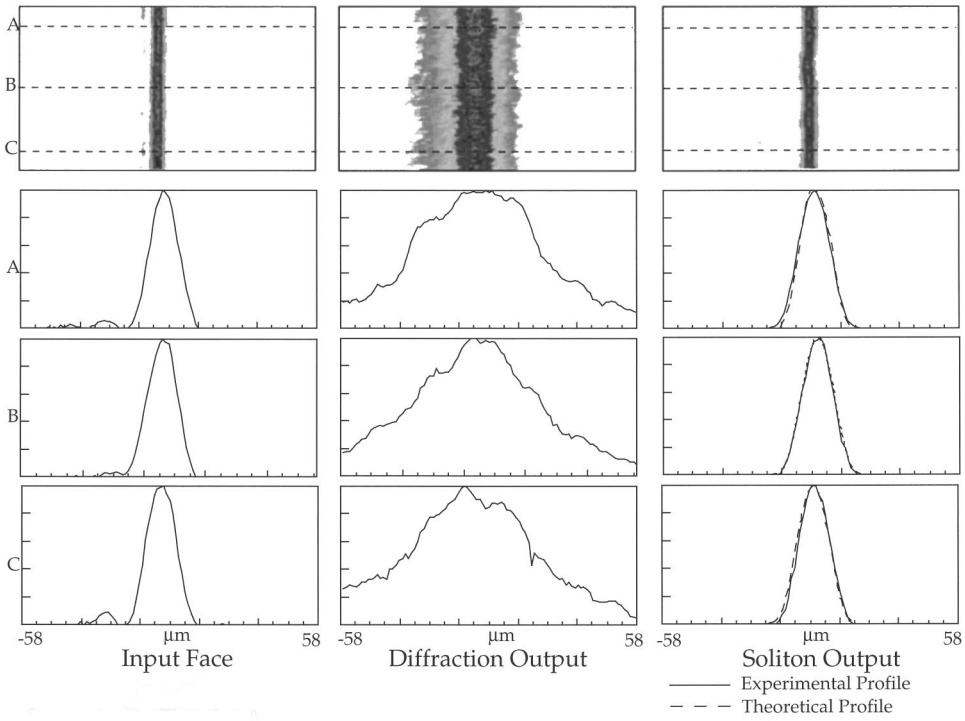

FIG. 1. One-dimensional photographs and profiles of a 14.5 μm input beam (left), the normally diffracting output (middle) and the soliton output beams (right) after propagating through a 6-mm SBN crystal. The profiles are taken at the planes marked by the dashed line on the photographs.

propagating along the crystalline **a** axis. A cylindrical lens is used to place the minimum waist of the one-dimensional Gaussian beam at the input face of the crystal. The input and output faces are imaged onto a charge-coupled-device camera with imaging resolution of ± 0.75 μm.

We generate solitons of various widths, typically between 9 and 20 μm (FWHM), at intensity ratios u_0^2 larger than 0.5. A typical observation of a 14.5-μm wide (FWHM) soliton, after propagating through the 6-mm length of the crystal, is shown in Fig. 1 This soliton had an amplitude ratio $u_0^2 = 7.6$ and required a voltage $V = 1.1$ kV applied along the **c** axis between electrodes spaced by 5 mm. With the voltage off the beam diffracts to about 56 μm. Using interferometry, we find that transverse phase profile at the exit face of the crystal is uniform. This implies that after leaving the crystal the soliton will propagate as if it had a minimal waist at the exit plane, and thus we use Gaussian-beam optics to image the output beam onto our camera. Photographs and beam profiles (taken at three different locations across the 1D beam) of the input beam (left), output diffracting beam at zero voltage (middle), and the output soliton beam (right) are shown in Fig. 1. We have examined the output beam profile across the entire 1D beam and found that, while the soliton output beam profiles do not change much (as shown on the right column), the diffracted output beam profiles (middle column) vary significantly from one plane to another and exhibit roughness caused by material defects and inhomogeneities. Hence, the appropriate voltage not only traps the beam, but also reshapes it to the smooth soliton wave form, which is largely unaffected by the crystal inhomogeneities.

Previous observations with photorefractive solitons [2,3,6] agree qualitatively with theory, but exact (quantitative) comparison was not possible. For one-dimensional screening solitons, however, we can measure all parameters necessary for a direct comparison. Measurement of the half-wave voltage, V_π, yields the product $n_b{}^3 r_{\rm eff} V_\pi / l$. Independent measurements of the electro-optic coefficient ($r_{33} = 194$ pm/volt) and the refractive index ($n_b = 2.35$) can then be used to infer that there is no significant voltage drop on the electrodes and that the entire voltage drops across the crystal (not on the electrodes). Values of $k^2 n_b{}^2 r_{\rm eff} V/l$, the peak soliton irradiance and the background irradiance completely determine the soliton solution of Eq. (2). We use this and $u_0^2 = 7.6$ to calculate the soliton profile at the experimental conditions of Fig. 1 and obtain the soliton profiles given by the dashed line in Fig. 1 (right column). We find good agreement between theory and experiment.

Next, we measure the soliton width as a function of the intensity ratio using the following procedure. We generate a soliton of a given width and measure the voltage required for trapping as a function of the intensity ratio. We repeat this experiment for solitons of widths ranging from 9 μm to 20 μm (FWHM) with the results shown in Fig. 2. Figure 2 also contains the theoretical result, which is a universal curve (solid). There is good qualitative agreement between the observations and the theory. The shapes of the individual data sets are in agreement with the theory and the minima lie at or slightly greater than the theoretical intensity ratio. Furthermore, in all our experiments and in the theory, a soliton of a specific width at a given value of intensity ratio, exists at a *single* value of V/l. Note also a recent experiment [8] that has measured the magnitude of the screening nonlinearity using *Z*-scan techniques and found the ''optimal photorefractive lens'' at an intensity ratio 4, which agrees well with both our theory [5] and the results presented in Fig. 2. There is, however, an obvious offset between the theoretical and the experimental results of Fig. 2 that appears to depend on the absolute value of the soliton width.

Several factors may explain the discrepancy between the measurements and the theory shown in Fig. 2: (1) higher order terms in the theory [5] that are omitted in the derivation of Eq. (1); (2) errors in the measurement of the electric

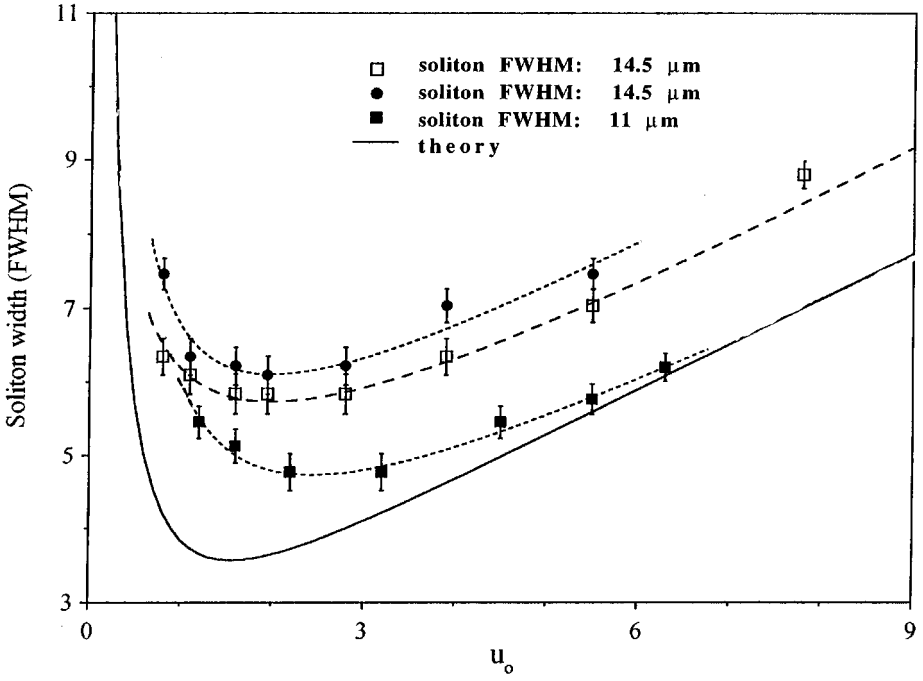

FIG. 2. Theoretical (solid) and experimental (dashed) plots of the soliton width in dimensionless units (ξ) as a function of u_0.

field; (3) random (local) variations in the electro-optic coefficient across the crystal; (4) dichroism that causes the extraordinary soliton beam to undergo different absorption from the ordinary background beam; and (5) guidance of the background beam by the soliton waveguide. Higher order terms do not appear to be the cause of the discrepancy because these should be more important for smaller soliton widths, contrary to the experimental results shown in Fig. 2. Since the electric field is independently found through a polarization-rotation experiment to be V/l, we infer field errors are not the cause. While the electro-optic coefficient varies across the crystal by about 10%, this is too small to cause the discrepancy shown in Fig. 2. The extraordinary and ordinary absorption coefficients are 1.55 and 1.65 cm^{-1}, respectively, but this changes the irradiance by at most 5%—again too small to explain the observed deviation. Guiding of the background beam is more difficult to estimate. The difference between the refractive index at the center and wings of the soliton is about 10^{-3} while that for the ordinarily polarized background beam is about 2×10^{-4}. This is sufficient to change the irradiance ratio locally, an effect which depends explicitly on the size of the soliton and on the angle between the soliton and the direction of propagation of the background beam. If both beams are exactly copropagating the background beam is partially guided by the soliton-induced waveguide. When the soliton and background beams differ in their propagation angles by an angle larger than the maximum guidance angle, the background beam cannot excite a guided mode of the waveguide and, as a result, the background beam is depleted in the center of the soliton. Both cases change the intensity ratio locally and we indeed observe them both in our experiments.

One-dimensional solitons may be unstable to perturbations in the direction of the soliton (ξ or x) and perpendicular to the soliton (y). They were found to be stable against perturbation in the x direction in Ref. [9] for a nonlinearity of the form $u^2/(1+u^2)$ and in Ref. [7] for photorefractive screening solitons. This agrees with our observations; if the external field appropriate for a soliton of a specific intensity ratio has a small ($\leqslant$10%) deviation from the single-value curve of Fig. 2 (which is equivalent to a perturbation in the x direction), the soliton is stable.

Stability against perturbations in the y direction is more complicated. For the Kerr nonlinearity, which is proportional to u^2, 1D solitons are unstable in a bulk material and break up into multiple filaments [10] (for this reason all bright Kerr solitons are observed in waveguides). The screening nonlinearity reduces to the Kerr nonlinearity in the limit of irradi-

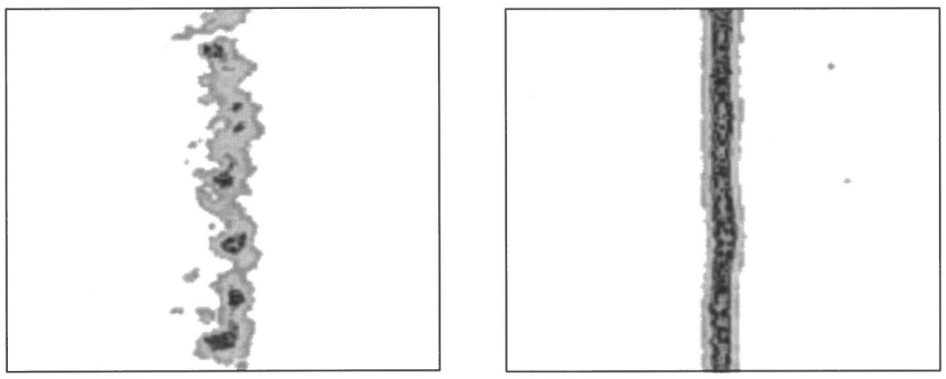

FIG. 3. Photographs of the stable 14.5 μm wide soliton output profile (right) for $u_0^2=7.6$, and the unstable (multiple-filament) beam (left) for $u_0^2=0.3$, after propagating through the 6mm long SBN crystal.

ance small compared to background plus dark irradiance [5] so one expects instability of the screening soliton in this regime. Recently, Zozulya and Anderson [11] claimed that one-dimensional screening solitons are unstable to perturbations in the *y* direction in all regimes.

We find experimentally that planar screening solitons in a weakly striated crystal of SBN do not break up into filaments unless their peak irradiance is smaller than the background irradiance. Typical photographs of the stable soliton with $u_0^2=7.6$ and an unstable multifilament beam with $u_0^2=0.3$ are shown in Fig. 3 (left and right pictures, respectively). The upper limit on the irradiance ratio at which we observe stable solitons is set by surface currents and breakdown that occur at the high voltages needed for large intensity ratios. The observed instability at low ratios may result from two sources. The first is connected with striations, which exist in all SBN crystals and spatially-modulate both the soliton and the background beams. Striations generally exist in the plane normal to the ferroelectric axis, thus they introduce perturbations in the *y* direction. The perturbations in the background beam affect the soliton more for $u_0^2 \ll 1$, and may be the reason for beam breakup. The second possible reason for instability at low intensity ratios is fundamental: *in this limit* ($u_0^2 \ll 1$) the 1D screening nonlinearity resembles the Kerr nonlinearity [5], where the instability of 1D solitons in a bulk material is inherent. For $u_0^2 > 1$ the solitons are stable as in saturable self-focusing media [12], or the perturbations have a much smaller growth coefficient in this regime such that instability is not observed in propagation through the 6-mm crystal. In general, the stability of the solitons always improves with increasing intensity ratio.

In conclusion, the one-dimensional theory gives good agreement with observations, and the screening solitons appear stable for propagation 0.6 cm in SBN when the peak-to-background intensity ratio is greater than one but break up into multiple filaments for smaller values.

M. Segev gratefully acknowledges the generous support of the Sloan Foundation and of Hughes Research Laboratories.

[1] M. Segev, B. Crosignani, A. Yariv, and B. Fischer, Phys. Rev. Lett. **68**, 923 (1992).

[2] G. Duree, J. L. Shultz, G. Salamo, M. Segev, A. Yariv, B. Crosignani, P. DiPorto, E. Sharp, and R. R. Neurgaonkar, Phys. Rev. Lett. **71**, 533 (1993); *ibid.* **74**, 1978 (1995).

[3] G. C. Valley, M. Segev, B. Crosignani, A. Yariv, M. M. Fejer, and M. Bashaw, Phys. Rev. A **50**, R4457 (1994); M. Taya, M. Bashaw, M. M. Fejer, M. Segev, and G. C. Valley, *ibid.* **52**, 3095 (1995).

[4] M. D. Iturbe-Castillo, P. A. Marquez-Aguilar, J. J. Sanchez-Mondragon, S. Stepanov, and V. Vysloukh, Appl. Phys. Lett. **64**, 408 (1994).

[5] M. Segev, G. C. Valley, B. Crosignani, P. DiPorto, and A. Yariv, Phys. Rev. Lett. **73**, 3211 (1994); M. Segev, M. Shih, and G. C. Valley, J. Opt. Soc. Am. **13**, 706 (1996).

[6] M. Shih, M. Segev, G. C. Valley, G. Salamo, B. Crosignani, and P. DiPorto, Elect. Lett. **31**, 826 (1995); M. Shih, P. Leach, M. Segev, M. Garrett, G. Salamo, and G. C. Valley, Opt. Lett. **21**, 324 (1996).

[7] S. R. Singh and D. N. Christodoulides, Opt. Commun. **118**, 569 (1995).

[8] P. A. Marquez-Aguilar, J. J. Sanchez-Mondragon, S. Stepanov, and G. Bloch, Opt. Commun. **118**, 165 (1995).

[9] S. Gatz and J. Herrmann, J. Opt. Soc. Am. B **8**, 2296 (1991).

[10] V. E. Zakharov and A. M. Rubenchik, JETP **38**, 494 (1974).

[11] A. Zozulya and D. Z. Anderson, in *Technical Digest of the Photorefractive Materials, Effects and Devices Topical Meeting*, (Optical Society of America, Washington, DC, 1995).

[12] M. Karlsson, Phys. Rev. A **46**, 2726 (1992).